Cherubism allele heterozygosity amplifies microbe-induced inflammatory responses in murine macrophages.

Virginie Prod'Homme, Laurent Boyer, Nicholas Dubois, Aude Mallavialle, Patrick Munro, Xavier Mouska, Isabelle Coste, Robert Rottapel, Sophie Tartare-Deckert, M. Deckert

Cherubism allele heterozygosity amplifies microbe-induced inflammatory responses in murine macrophages

Virginie Prod'Homme,[1,2] Laurent Boyer,[2,3] Nicholas Dubois,[1,2] Aude Mallavialle,[1,2] Patrick Munro,[2,3] Xavier Mouska,[2] Isabelle Coste,[4] Robert Rottapel,[5] Sophie Tartare-Deckert,[1,2] and Marcel Deckert[1,2]

[1]INSERM, U1065, Centre Méditerranéen de Médecine Moléculaire (C3M), Microenvironment, Signaling and Cancer, Nice, France. [2]Université de Nice Sophia-Antipolis, Faculté de Médecine, Nice, France. [3]INSERM, U1065, C3M, Microbial Toxins in Host Pathogen Interactions, Nice, France. [4]Cancer Research Center Lyon, UMR INSERM 1052, CNRS 5286, Lyon, France. [5]Ontario Cancer Institute, Toronto Medical Discovery Tower, Toronto, Ontario, Canada.

Cherubism is a rare autoinflammatory bone disorder that is associated with point mutations in the SH3-domain binding protein 2 (*SH3BP2*) gene, which encodes the adapter protein 3BP2. Individuals with cherubism present with symmetrical fibro-osseous lesions of the jaw, which are attributed to exacerbated osteoclast activation and defective osteoblast differentiation. Although it is a dominant trait in humans, cherubism appears to be recessively transmitted in mice, suggesting the existence of additional factors in the pathogenesis of cherubism. Here, we report that macrophages from 3BP2-deficient mice exhibited dramatically reduced inflammatory responses to microbial challenge and reduced phagocytosis. 3BP2 was necessary for LPS-induced activation of signaling pathways involved in macrophage function, including SRC, VAV1, p38MAPK, IKKα/β, RAC, and actin polymerization pathways. Conversely, we demonstrated that the presence of a single *Sh3bp2* cherubic allele and pathogen-associated molecular pattern (PAMP) stimulation had a strong cooperative effect on macrophage activation and inflammatory responses in mice. Together, the results from our study in murine genetic models support the notion that infection may represent a driver event in the etiology of cherubism in humans and suggest limiting inflammation in affected individuals may reduce manifestation of cherubic lesions.

Introduction

Cherubism is a rare genetic bone dysplasia characterized by symmetrical jawbone lesions causing severe facial and dental deformity and associated with mutations of the SH3-domain binding protein 2 (*SH3BP2*) gene. The most frequent *SH3BP2* mutations affect exon 9, leading to the substitution of amino acids Arg415, Pro418, or Gly420 within an RSPPDG motif of the protein 3BP2 (1–3). 3BP2 is a cytoplasmic adapter involved in leukocyte activation (4–7), osteoclast differentiation, and bone remodeling (8, 9). 3BP2 signals downstream of diverse leukocyte membrane receptors through interactions with SRC and SYK kinases, PLCγ, and VAV GEF (2, 3).

Determinant insights into the mechanism underlying cherubism came from the analysis of the *Sh3bp2*^{P416R} genetic mouse model of cherubism (10). Whereas heterozygous cherubic mice showed no significant phenotype, homozygous cherubic animals developed systemic inflammation and severe osteopenia (10, 11). This phenotype has been linked to exacerbated activities of intracellular signaling components resulting from the accumulation of proteasome-resistant mutant 3BP2 proteins in mouse osteoclasts (12).

However, several aspects of cherubism are still unclear, including the craniofacial manifestation, the variable penetrance, and its mode of transmission. Whereas the disease is dominantly transmitted in humans, it is recessively transmitted in cherubic mouse models housed under germ-free conditions. Together, these aspects suggest that additional genetic or environmental factor or factors may influence the onset of the disease. Microbial infections of the oral cavity dramatically affect local inflammation and subsequent bone-destructive diseases, such as periodontitis (13). We thus hypothesized that pathogenic microbial challenge may contribute to the development of the cherubism phenotype by exacerbating inflammatory responses of host macrophages. Here, we demonstrate that 3BP2 deficiency in the mouse alters macrophage responses to microbial stimuli. Conversely, we show that TLR stimulation and one *Sh3bp2* cherubic allele have a dramatic cooperative effect on macrophage activation and inflammatory responses. Our study in mice suggests that microbial infection participates in the development of cherubism in humans, thereby opening new therapeutic avenues.

Results and Discussion

In mice, homozygosity for a cherubism mutation in *Sh3bp2* caused an autoinflammatory syndrome initiated by macrophages producing high levels of TNF-α (10). Because macrophages are important components of the innate immune system involved in pathogen recognition (14), we hypothesized that infection may contribute to the onset of the disease in humans. To test this hypothesis, we first determined the dependence of TLR stimulation by pathogen-associated molecular patterns (PAMPs) on 3BP2 expression

Conflict of interest: The authors have declared that no conflict of interest exists.
Submitted: December 1, 2014; **Accepted:** January 8, 2015.
Reference information: *J Clin Invest*. doi:10.1172/JCI71081.

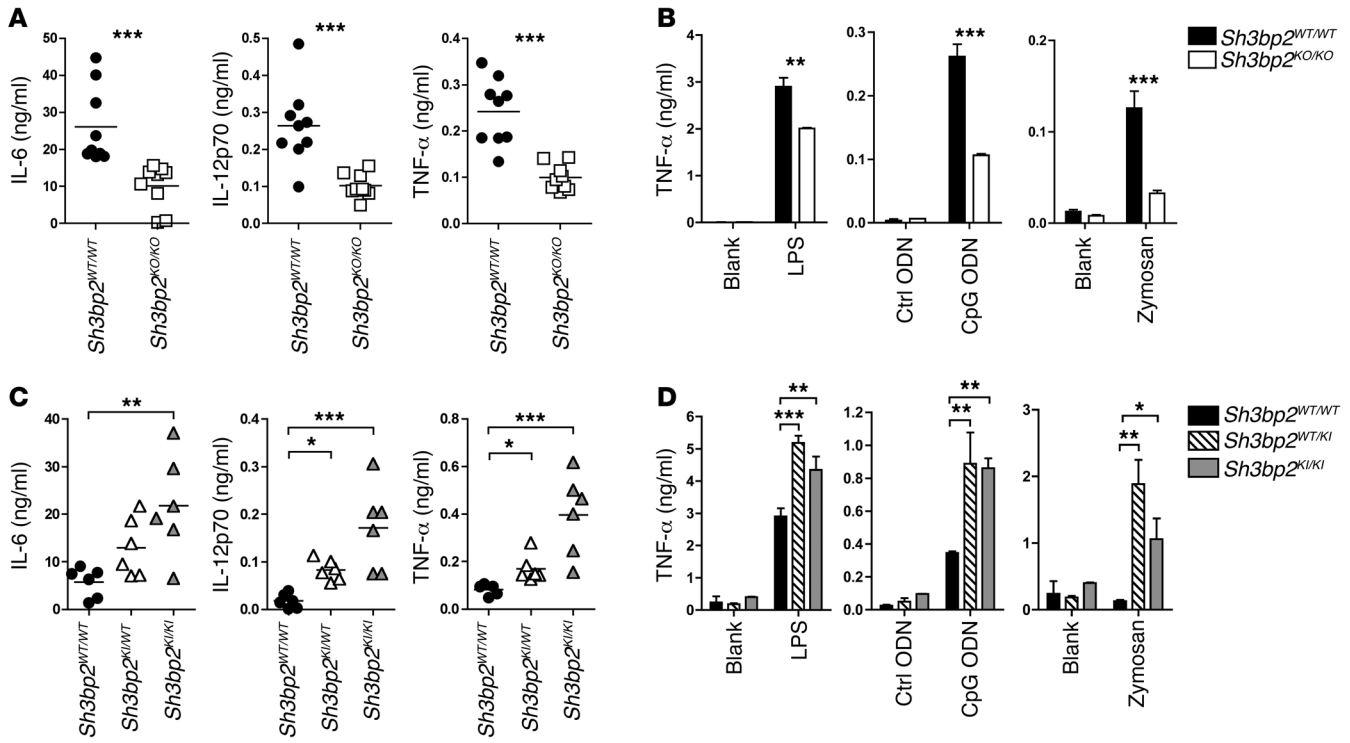

Figure 1. Macrophages from 3BP2-deficient and cherubic mice display impaired cytokine response to PAMP challenge. (**A** and **C**) Mice were injected i.p. with LPS, and cytokines in the serum were measured by ELISA 4 hours later. (**B** and **D**) BMM were stimulated in vitro with LPS, zymosan depleted of TLR-stimulating properties, or CpG ODN (n = 3). TNF-α was measured in supernatant by ELISA. P values shown were determined by the following tests: 2-tailed Mann-Whitney U test (**A**); 2-way ANOVA (**B** and **D**); Kruskal-Wallis test (**C**). $^*P < 0.05$; $^{**}P < 0.01$; $^{***}P < 0.001$.

in mice. In response to in vivo LPS challenge, reduced levels of inflammatory cytokines (IL-6, IL-12p70, and TNF-α) were measured in the serum of *Sh3bp2*$^{KO/KO}$ mice compared with WT animals (*Sh3bp2*$^{WT/WT}$) (Figure 1A), suggesting that 3BP2 is essential for the inflammatory function of macrophages. As a control, analysis of the number and phenotype of blood monocytes and spleen macrophages in WT and *Sh3bp2*$^{KO/KO}$ mice indicated that 3BP2 was dispensable for proliferation and differentiation of monocytes and macrophages under steady-state conditions (Supplemental Figure 1; supplemental material available online with this article; doi:10.1172/JCI71081DS1). Importantly, macrophage recruitment to the peritoneal cavity in response to LPS or thioglycolate injections was unaffected in *Sh3bp2*$^{KO/KO}$ mice (Supplemental Figure 2). Adoptive transfer of thioglycolate-elicited peritoneal WT and *Sh3bp2*$^{KO/KO}$ macrophages into macrophage-depleted mice followed by in vivo LPS stimulation further demonstrated that the defect in inflammatory reaction was intrinsic to *Sh3bp2*$^{KO/KO}$ macrophages (Supplemental Figure 3). To confirm the role of 3BP2 in macrophage, BM-derived macrophages (BMM) were generated in vitro and challenged with bona fide PAMP: LPS, CpG oligodeoxynucleotide (CpG ODN), or zymosan depleted of TLR-stimulating properties. The concentration of TNF-α in the supernatant of *Sh3bp2*$^{KO/KO}$ BMM was reduced in response to all 3 stimuli, suggesting that in addition to TLR signaling, 3BP2 deficiency also affects DECTIN1 signaling (Figure 1B). Note that expression of TLR4, TLR9, and DECTIN1, receptors for LPS, CpG ODN, and zymosan, respectively, was unchanged on *Sh3bp2*$^{KO/KO}$ macrophages (Supplemental Figure 1, D and E). Also, LPS-stimulated BM-derived DC (BM-DC) from WT and *Sh3bp2*$^{KO/KO}$ mice produced similar levels of IL-12p70 (Supplemental Figure 4), indicating that 3BP2 is not required for DC stimulation.

To determine the impact of microbial stimulation on cherubic macrophage, we used gene targeting to introduce into the murine *Sh3bp2* gene the mutation Gly418Arg (Supplemental Figure 5), equivalent to the Gly420Arg mutation frequently found in cherubic patients (1). The phenotype of homozygous *Sh3bp2*^{G418R} (*Sh3bp2*$^{KI/KI}$) mice was strikingly similar to that described for homozygous *Sh3bp2*^{P416R} mice, another cherubic mutant mouse generated by Ueki et al. (10), with typical facial swelling associated with eyelid closure, bone loss, lymphadenopathy, monocytosis, and systemic inflammation, as revealed by constitutive high levels of inflammatory cytokines in *Sh3bp2*$^{KI/KI}$ mouse serum (Supplemental Figure 6). In addition, we observed that 3BP2 Gly418Arg mutant proteins accumulated in BMM (Supplemental Figure 6F). In contrast, heterozygous mice (*Sh3bp2*$^{WT/KI}$) showed no gross abnormalities under germ-free housing conditions. However, a significant increase of inflammatory cytokines was detected in the serum of both *Sh3bp2*$^{WT/KI}$ and *Sh3bp2*$^{KI/KI}$ mice challenged with LPS (Figure 1C). When stimulated in vitro with LPS, CpG ODN, or zymosan, TNF-α production by *Sh3bp2*$^{WT/KI}$ and *Sh3bp2*$^{KI/KI}$ BMM was enhanced compared with that of WT BMM (Figure 1D). Furthermore, heterozygous cherubic mice (*Sh3bp2*$^{WT/KI}$) infected with high doses of *E. coli* were more sensitive to septic shock (Supplemental Figure 6, G and H). These observations suggest that the association between a single cherubism allele and the PAMP challenge is sufficient to reach pathogenic levels of inflammatory cytokines.

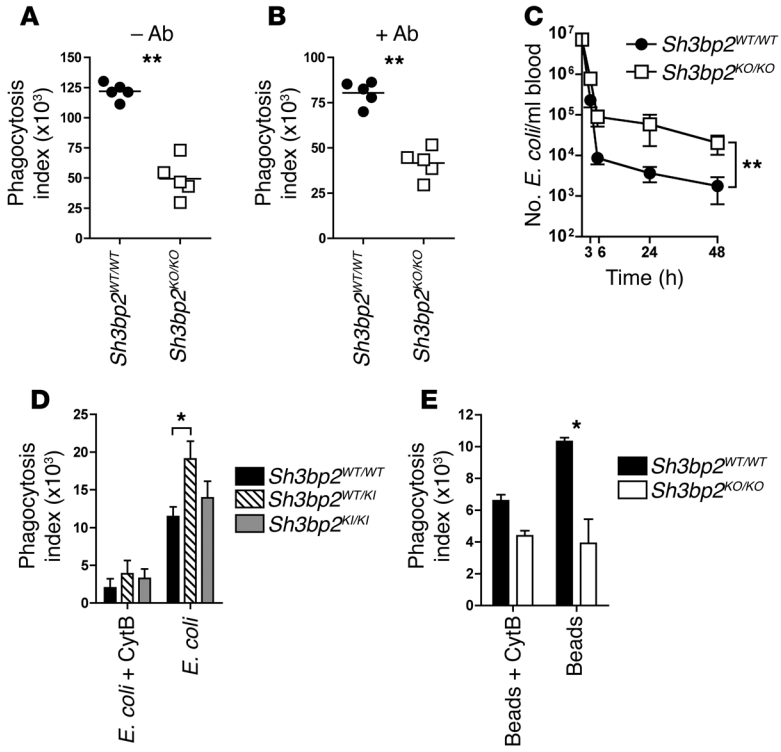

Figure 2. Macrophages from 3BP2-deficient and cherubic mice display impaired phagocytosis. BMM were incubated 10 minutes with *E. coli*–FITC ($n = 5$) (**A**) or Ab-opsonized *E. coli*–FITC ($n = 5$) (**B**), and intracellular fluorescence was analyzed by flow cytometry. (**C**) 10^7 *E. coli* bacteria were injected in the mouse tail veins. Blood samples were harvested 3, 6, 24, and 48 hours after injection, and the number of bacteria per ml of blood was counted after 16 hours culture on LB-agar ($n = 14$). (**D**) BMM were incubated 10 minutes with *E. coli*–FITC ($n = 3$), and intracellular fluorescence was analyzed by flow cytometry. (**E**) BMM were incubated with latex fluorescent beads ($n = 4$). Cytochalasin B (CytB) was added to inhibit phagocytosis in control wells. *P* values were determined by the following tests: 2-tailed Mann-Whitney *U* test (**A** and **B**); 2-way ANOVA (**C**–**E**). $^*P < 0.05$; $^{**}P < 0.01$.

We next investigated the role of 3BP2 in macrophage phagocytosis. In vitro phagocytosis assays with nonopsonized and Ab-opsonized fluorescent *E. coli* showed that 3BP2 was required for both Ab-dependent and -independent phagocytosis (Figure 2, A and B). Consistently, in vivo *E. coli* clearance was less efficient in $Sh3bp2^{KO/KO}$ animals (Figure 2C). Conversely, phagocytic capacity of heterozygous cherubic BMM was exacerbated compared with that of WT macrophages (Figure 2D). TLR and Fc receptors signal via different cytosolic molecular pathways (14, 15), and 3BP2 has been implicated in a variety of membrane receptor signaling pathways, including those stimulated by immunoreceptors (4, 5), RANK (8), and GPCR (16). Therefore, it seems unlikely that 3BP2 interacts with specific regulators of either TLR or Fc receptor pathways in macrophages. Indeed, $Sh3bp2^{KO/KO}$ BMM were also ineffective in phagocyting latex beads (Figure 2E).

Our observations thus indicate that 3BP2 function during pathogen recognition by macrophages is related to a general cellular process. The necessity of actin cytoskeleton remodeling during phagocytosis is well known (17). Consistently, the increased activity of *E. coli* engulfment observed in heterozygous cherubic BMM was blocked by the actin-depolymerizing drug cytochalasin B (Figure 2D). 3BP2-mediated signaling in leukocyte involved interactions with SRC and SYK kinases and VAV GEF (2), which control gene transcription and cytoskeletal changes in stimulated macrophages (18, 19). Accordingly, 3BP2 bound SRC and VAV1 in BMM extracts (Figure 3A). Upon LPS stimulation, phosphorylation of SRC and VAV1 was reduced in $Sh3bp2^{KO/KO}$ BMM, along with activation of signaling proteins required for inflammatory cytokine production, including JNK1/2, p38, and IKKα/β (Figure 3B). Absence of 3BP2 in resting and LPS-stimulated macrophages also reduced RAC activity (Figure 3D) and actin polymerization (Figure 3E). In addition, LPS-induced actin polymerization was diminished in $Sh3bp2^{KO/KO}$ peritoneal macrophages, but not DC (Supplemental Figure 7), and $Sh3bp2^{KO/KO}$ BMM were impaired in their capacity to differentiate into multinucleated osteoclasts (Supplemental Figure 8). Importantly, cytochalasin B decreased IL-6 production by LPS-stimulated WT macrophages (32% of reduction compared with untreated LPS-stimulated cells). This effect was more pronounced in $Sh3bp2^{KO/KO}$ macrophages (68% of reduction compared with untreated LPS-stimulated cells) (Table 1). Further supporting the notion that actin dynamics in macrophage is a key event downstream of 3BP2, IL-6 secretion by LPS-stimulated $Sh3bp2^{KO/KO}$ BMM was restored to normal levels by the actin-polymerizing agent jasplakinolide (Table 1). We next determined how these 3BP2-associated signaling pathways were affected in cherubic BMM. When compared with WT macrophages, unstimulated homozygous cherubic macrophages exhibited constitutive levels of phosphorylation of several signaling components, including p38, SRC, and VAV1 (Figure 3C), and of RAC activity (Figure 3D), a phenomenon likely related to the autoinflammatory condition of these cells. Strikingly, depleting the commensal microbiota with oral antibiotic treatment did not decrease the inflammation in homozygous cherubic mice (Supplemental Figure 9). However, in agreement with a recent study (20), crossing $Sh3bp2^{KI/KI}$ mice with $Myd88^{KO/KO}$ mice reduced serum TNF-α to WT levels, demonstrating the involvement of TLR signaling in autoinflammation of homozygous cherubic mice (Figure 3F). Most importantly, LPS-stimulated heterozygous cherubic BMM displayed enhanced signaling activities compared with WT macrophages (Figure 3, C and D), and heterozygous cherubic mice ($Sh3bp2^{WT/KI}$) orally treated with chronic LPS stimulation presented serum TNF-α levels similar to those found in untreated homozygous cherubic mice (Figure 3G and Supplemental Figure 6E). Our results in mouse models of normal and pathological 3BP2 function indicate that a complex between 3BP2, SRC, and VAV1 may bridge pathogen recognition to RAC activation and actin cytoskeleton remodeling, key processes of macrophage functions. In support of this notion, activation of small RHO GTPases has been recently recognized as a process induced by cytosolic microbial products detected by NOD1 (21). Finally, our data reveal that an increased threshold of TLR signaling, and potentially of other PAMP receptors, associated with monoallelic *SH3BP2* mutation may exacerbate macrophage sensitivity to microbial stimuli in cherubism-affected individuals. Upon oral infection, this aberrant process would hence initiate a

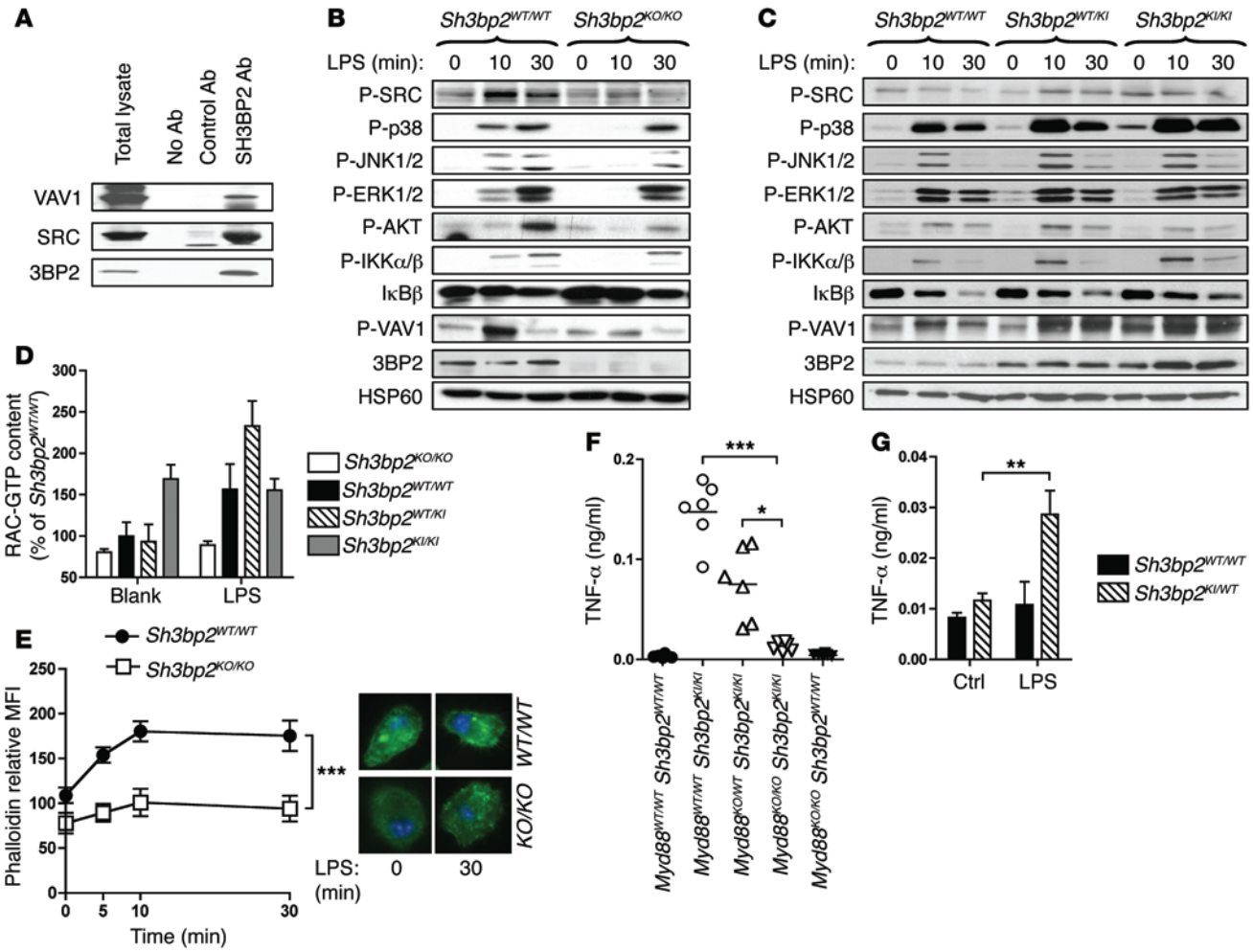

Figure 3. TLR4 signaling is impaired in macrophages from 3BP2-deficient and cherubic mice. (**A**) Lysates from *Sh3bp2*$^{WT/WT}$ BMM were immunoprecipitated with protein G–sepharose beads coated with control Abs, anti-3BP2 Abs, or no Abs and immunoblotted using the indicated Abs. (**B** and **C**) Immunoblot analysis and (**D**) measurement of RAC activity by G-LISA were performed on cell lysates of BMM stimulated with LPS for the indicated times. (**E**) LPS-stimulated BMM were stained with fluorescent phalloidin and analyzed by flow cytometry (n = 3). Representative microscopic pictures of phalloidin and DAPI-stained BMM, either untreated (left) or stimulated with LPS for 30 minutes (right), are shown. (**F**) TNF-α was measured by ELISA in the serum of untreated mice (n = 6). (**G**) LPS was added for 28 days in mouse drinking water, and TNF-α in the serum was measured by ELISA (n = 6). P values were determined by the following tests: 2-way ANOVA (**D**, **E** and **G**); (Kruskal-Wallis test (**F**). *P < 0.05; **P < 0.01; ***P < 0.001.

pathological inflammation responsible for the cherubic lesions in humans. Clinically, our study suggests new therapeutic options to reduce the manifestations of the genetic disease cherubism.

Methods

Further information is available in Supplemental Methods.

Mice and in vivo experiments. Mice were on a C57BL/6 background. *Sh3bp2*$^{KO/KO}$ (6) and *Myd88*$^{KO/KO}$ (22) mice have been described. Cherubic mice were generated by the Institut Clinique de la Souris (ICS) by knocking-in (KI) the GGA-to-CGA mutation in the *Sh3bp2* exon 9, resulting in a Gly418-to-Arg substitution in 3BP2 protein (Supplemental Figures 5 and 6 and Supplemental Methods). In vivo experiments were performed on 8- to 12-week-old mice as described in Supplemental Methods.

BMM differentiation and in vitro assays. Cells were flushed out of mouse femurs and tibias and cultured for 5 to 7 days at 37°C, 5% CO_2, in RPMI, 50 U/l penicillin, 50 μg/l streptomycin, 1 mM sodium pyruvate, 10 μM HEPES, 10% FBS, and 50 ng/ml M-CSF. BMM were stimulated for 16 hours with LPS (*E. coli* strain 055:B5, Sigma-Aldrich) or CpG ODN (Invivogen) in the presence of 2 μM cytochalasin B or 0.5 μM jasplakinolide (Sigma-Aldrich). Cytokines in supernatants were measured by ELISA (eBioscience). For phagocytosis assay, 5 × 10^6 FITC–*E. coli* (Life Technologies) or 10^7 red fluorescent–latex

Table 1. Impact of actin polymerization drugs on cytokine secretion by LPS-stimulated BMM

	Sh3bp2$^{WT/WT}$	*Sh3bp2*$^{KO/KO}$	*P* values
Blank	10.5 ± 3.6	13.3 ± 3	P > 0.05
LPS	661.5 ± 8.6	492.4 ± 1.2	P < 0.01
LPS + cytochalasin B	450.5 ± 20.7	159.1 ± 2.8	P < 0.001
LPS + jasplakinolide	963.6 ± 56.2	648.6 ± 43.4	P < 0.001

BMM were stimulated in vitro with 100 ng/ml LPS in the presence of cytochalasin B (2 μM) or jasplakinolide (0.5 μM) for 16 hours. Results are shown as mean ± SEM of the IL-6 concentration (pg/ml) measured in cell supernatants by ELISA.

beads (Sigma-Aldrich) were centrifuged on 10^6 BMM/well and incubated at 37°C for 10 minutes. BMM pretreatment with cytochalasin B was used to inhibit phagocytosis. In some experiments, bacteria were opsonized (BioParticles opsonizing reagent, Life Technologies) prior to incubation with macrophages. BMM were washed and fixed in 1% PFA for 30 minutes. Extracellular fluorescence was quenched with trypan blue, and intracellular fluorescence was evaluated by flow cytometry. The phagocytosis index was calculated as follows: (percentage of fluorescent BMM × MFI of fluorescent BMM)/MFI BMM incubated without particles.

F-actin staining and RAC assay. Cells were treated with fixation and permeabilization buffers (eBioscience), stained with Alexa Fluor 488 phalloidin (Life Technologies), and analyzed by flow cytometry. Alternatively, polymerized actin was analyzed using a Zeiss Axiovert fluorescence microscope, as described before (8). RAC activities were measured on BMM lysates using G-LISA RAC Activation Assays (Cytoskeleton). Data are the mean ± SEM of arbitrary units of RAC1/2/3 activity and are represented as the percentage of RAC activity in untreated WT cells.

Immunoblotting and IP. Immunoblotting and co-IP were performed on BMM lysates as described (8). Abs were as follows: rabbit and goat Abs against 3BP2 (5, 8); Abs against phosphorylated forms of SRC, SYK, ERK1/2, p38, JNK1/2, AKT, IKKα/β, IκBα (Cell Signaling Technology); anti–p-VAV1, and ERK2 (Santa Cruz Biotechnology Inc.).

Statistics. Statistical data analysis was performed with Prism (GraphPad Software) without assuming Gaussian distribution. Data represent mean ± SEM. Mann-Whitney *U* tests were used for statistical comparisons between 2 groups and Kruskal-Wallis tests with Dunn's post-tests or 2-way ANOVA tests with Bonferroni's post-tests to compare 3 or more groups. $P < 0.05$ was considered significant.

Study approval. Mouse experiments were approved by the Institutional Animal Care and Use committee of the University of Nice Sophia-Antipolis.

Acknowledgments

This study is dedicated to Alain Bernard. This work was supported by INSERM, the Agence National de la Recherche (ANR) through the program ANR-06-MRAR-013-01 and the "Investments for the Future" LABEX SIGNALIFE ANR-11-LABX-0028-01, and by grants from the Fondation pour la Recherche Médicale and the Fondation de France (to V. Prod'Homme). The mouse mutant line *Sh3bp2*$^{KI/WT}$ was established at ICS with funds from ANR-MRAR. We thank S. Akira (Osaka University, Osaka, Japan) for *Myd88*$^{KO/KO}$ mice, N. Van Rooijen (Vrije University, Amsterdam, The Netherlands) for liposome-encapsulated clodronate, E. Lemichez (INSERM, Nice, France) for the *E. coli* strain UTI-89, and N. Rochet (INSERM, Nice, France) for radiography of cherubic mice.

Address correspondence to: Marcel Deckert, INSERM U1065, C3M, Team 11, Bâtiment Universitaire Archimed, 151 Route Saint-Antoine de Ginestière, BP 2 3194, 06204 Nice Cedex 3, France. Phone: 33.489.064.310; E-mail: deckert@unice.fr.

1. Ueki Y, et al. Mutations in the gene encoding c-Abl-binding protein SH3BP2 cause cherubism. *Nat Genet*. 2001;28(2):125–126.
2. Deckert M, Rottapel R. The adapter 3BP2: how it plugs into leukocyte signaling. *Adv Exp Med Biol*. 2006;584:107–114.
3. Reichenberger EJ, Levine MA, Olsen BR, Papadaki ME, Lietman SA. The role of SH3BP2 in the pathophysiology of cherubism. *Orphanet J Rare Dis*. 2012;7(suppl 1):S5.
4. Deckert M, Tartare-Deckert S, Hernandez J, Rottapel R, Altman A. Adaptor function for the Syk kinases-interacting protein 3BP2 in IL-2 gene activation. *Immunity*. 1998;9(5):595–605.
5. Foucault I, Le Bras S, Charvet C, Moon C, Altman A, Deckert M. The adaptor protein 3BP2 associates with VAV guanine nucleotide exchange factors to regulate NFAT activation by the B-cell antigen receptor. *Blood*. 2005;105(3):1106–1113.
6. Chen G, et al. The 3BP2 adapter protein is required for optimal B-cell activation and thymus-independent type 2 humoral response. *Mol Cell Biol*. 2007;27(8):3109–3122.
7. Hatani T, Sada K. Adaptor protein 3BP2 and cherubism. *Curr Med Chem*. 2008;15(6):549–554.
8. GuezGuez A, et al. 3BP2 Adapter protein is required for receptor activator of NFκB ligand (RANKL)-induced osteoclast differentiation of RAW264.7 cells. *J Biol Chem*. 2010;285(27):20952–20963.
9. Levaot N, et al. 3BP2-deficient mice are osteoporotic with impaired osteoblast and osteoclast functions. *J Clin Invest*. 2011;121(8):3244–3257.
10. Ueki Y, et al. Increased myeloid cell responses to M-CSF and RANKL cause bone loss and inflammation in SH3BP2 "cherubism" mice. *Cell*. 2007;128(1):71–83.
11. Wang CJ, et al. Pro416Arg cherubism mutation in Sh3bp2 knock-in mice affects osteoblasts and alters bone mineral and matrix properties. *Bone*. 2010;46(5):1306–1315.
12. Levaot N, et al. Loss of Tankyrase-mediated destruction of 3BP2 is the underlying pathogenic mechanism of cherubism. *Cell*. 2011;147(6):1324–1339.
13. Graves DT, Li J, Cochran DL. Inflammation and uncoupling as mechanisms of periodontal bone loss. *J Dent Res*. 2011;90(2):143–153.
14. Kawai T, Akira S. Toll-like receptors and their crosstalk with other innate receptors in infection and immunity. *Immunity*. 2011;34(5):637–650.
15. Underhill DM, Goodridge HS. The many faces of ITAMs. *Trends Immunol*. 2007;28(2):66–73.
16. Chen G, et al. The 3BP2 adapter protein is required for chemoattractant-mediated neutrophil activation. *J Immunol*. 2012;189(5):2138–2150.
17. Bokoch GM. Regulation of innate immunity by Rho GTPases. *Trends Cell Biol*. 2005;15(3):163–171.
18. Berton G, Mocsai A, Lowell CA. Src and Syk kinases: key regulators of phagocytic cell activation. *Trends Immunol*. 2005;26(4):208–214.
19. Miletic AV, et al. Vav proteins control MyD88-dependent oxidative burst. *Blood*. 2007;109(8):3360–3368.
20. Yoshitaka T, et al. Enhanced TLR-MYD88 signaling stimulates autoinflammation in SH3BP2 cherubism mice and defines the etiology of cherubism. *Cell Rep*. 2014;8(6):1752–1766.
21. Keestra AM, et al. Manipulation of small Rho GTPases is a pathogen-induced process detected by NOD1. *Nature*. 2013;496(7444):233–237.
22. Kawai T, Adachi O, Ogawa T, Takeda K, Akira S. Unresponsiveness of MyD88-deficient mice to endotoxin. *Immunity*. 1999;11(1):115–122.